

Research Article

Reduced expression of cardiac ryanodine receptor protects against stress-induced ventricular tachyarrhythmia, but increases the susceptibility to cardiac alternans

Xiaowei Zhong^{1,*}, Alexander Vallmitjana², Bo Sun^{1,†}, Zhichao Xiao¹, Wenting Guo^{1,*}, Jinhong Wei^{1,‡}, Mingke Ni¹, Yongxiang Chen¹, Edward R. O'Brien¹, Anne M. Gillis¹, Masahiko Hoshijima³, Hiroshi Takeshima⁴, Leif Hove-Madsen⁵, Raul Benitez², Darrell Belke¹ and S.R. Wayne Chen^{1§}

¹The Libin Cardiovascular Institute of Alberta, Department of Physiology and Pharmacology, University of Calgary, Calgary, Alberta, Canada T2N 4N1; ²Department of Automatic Control, Universitat Politècnica de Catalunya, Barcelona 08034, Spain; ³Department of Medicine and Center for Research in Biological Systems, University of California, San Diego, CA 92093, U.S.A.; ⁴Department of Biological Chemistry, Graduate School of Pharmaceutical Sciences, Kyoto University, Kyoto 606-8501, Japan; ⁵Biomedical Research Institute of Barcelona (IIBB), CSIC, Sant Pau, Hospital de Sant Pau, Barcelona 08025, Spain

Correspondence: S.R. Wayne Chen (swchen@ucalgary.ca)

*X.Z. and W.G. are recipients of the Alberta Innovates — Health Solutions (AIHS) Studentship Award.

[†]B.S. is a recipient of the Heart and Stroke Foundation of Canada Junior Fellowship Award and the Alberta Innovates — Health Solutions (AIHS) Fellowship Award.

[‡]J.W. is a recipient of the Libin Cardiovascular Institute of Alberta and Cumming School of Medicine Postdoctoral Fellowship Award.

[§]S.R.W.C. is an AIHS scientist.

Received: 10 August 2017

Revised: 8 November 2017

Accepted: 22 November 2017

Accepted Manuscript online:
23 November 2017

Version of Record published:
5 January 2018

Reduced protein expression of the cardiac ryanodine receptor type 2 (RyR2) is thought to affect the susceptibility to stress-induced ventricular tachyarrhythmia (VT) and cardiac alternans, but direct evidence for the role of RyR2 protein expression in VT and cardiac alternans is lacking. Here, we used a mouse model (*crr*^{m1}) that expresses a reduced level of the RyR2 protein to determine the impact of reduced RyR2 protein expression on the susceptibility to VT, cardiac alternans, cardiac hypertrophy, and sudden death. Electrocardiographic analysis revealed that after the injection of relatively high doses of caffeine and epinephrine (agents commonly used for stress test), wild-type (WT) mice displayed long-lasting VTs, whereas the *crr*^{m1} mutant mice exhibited no VTs at all, indicating that the *crr*^{m1} mutant mice are resistant to stress-induced VTs. Intact heart Ca²⁺ imaging and action potential (AP) recordings showed that the *crr*^{m1} mutant mice are more susceptible to fast-pacing induced Ca²⁺ alternans and AP duration alternans compared with WT mice. The *crr*^{m1} mutant mice also showed an increased heart-to-body-weight ratio and incidence of sudden death at young ages. Furthermore, the *crr*^{m1} mutant hearts displayed altered Ca²⁺ transients with increased time-to-peak and decay time (T_{50}), increased ventricular wall thickness and ventricular cell area compared with WT hearts. These results indicate that reduced RyR2 protein expression suppresses stress-induced VTs, but enhances the susceptibility to cardiac alternans, hypertrophy, and sudden death.

Introduction

Ryanodine receptor type 2 (RyR2) is the major Ca²⁺ release channel expressed in the sarcoplasmic reticulum (SR) of cardiac muscle cells. It plays an essential role in excitation–contraction coupling by governing SR Ca²⁺ release, which causes muscle contraction [1]. Given its important role in cardiac function, dysfunction of RyR2 can lead to various cardiac disorders. Indeed, a large number of naturally occurring mutations in RyR2 have been associated with catecholaminergic polymorphic ventricular tachycardia (CPVT), atrial or ventricular fibrillation, hypertrophic or dilated cardiomyopathies, and sudden cardiac arrest [2,3]. RyR2 dysfunction as a result of abnormal post-translational modifications have also been implicated in various cardiac conditions, such as heart failure [4–6]. Although the molecular mechanisms by which RyR2 mutations and post-translational modifications cause

diseases are not completely understood, it is generally believed that most of these RyR2 mutations or modifications alter channel activation or inactivation, leading to enhanced or suppressed RyR2 activity [2,5–12].

Besides alterations in the activation or inactivation properties of the channel, changes in the protein expression of RyR2 have also been implicated in the pathogenesis of cardiac diseases [13–16]. It has been shown that the level of RyR2 protein expression is significantly increased in patients with paroxysmal atrial fibrillation (AF) and in a mouse model of AF [17,18]. These observations suggest that enhanced protein expression of RyR2 may be associated with an increased susceptibility to AF. On the other hand, ablating the expression of RyR2 by gene-targeted knockout (KO) resulted in embryonic lethality [19], while heart-specific, conditional KO of RyR2 led to cardiac hypertrophy and sudden death [20]. Reduced RyR2 protein expression has also been proposed to be involved in cardiac alternans. Wan et al. [21] showed that endocardial myocytes, which express less RyR2 and sarco/endoplasmic reticulum Ca^{2+} ATPase 2a (SERCA2a) proteins, are more susceptible to cardiac alternans than epicardial myocytes, which express higher levels of RyR2 and SERCA2a proteins. Furthermore, reduction in RyR2 protein expression may affect the susceptibility to stress-induced ventricular arrhythmias. Some CPVT-linked RyR2 mutations, such as the deletion of exon-3 and the point mutation G357S, were found to markedly reduce the expression of the RyR2 protein [22–24]. Interestingly, the clinical phenotypes and severities of individuals carrying these mutations appear to be highly variable, and some of them are even asymptomatic [23,25–28]. These observations suggest that reduced RyR2 protein expression may contribute to the incomplete penetrance of CPVT phenotypes. However, it is important to note that despite their potential association, direct evidence for the link between reduced RyR2 protein expression and CPVT susceptibility or cardiac alternans has yet to be established.

In the present study, we employed a mouse model [19] in which the protein expression of the wild-type (WT) RyR2 is substantially reduced to investigate the impact of reduced RyR2 protein expression on CPVT, cardiac alternans, cardiac hypertrophy, and sudden death. We demonstrated for the first time that reducing the level of the RyR2 protein protects against CPVT, but enhances the susceptibility to Ca^{2+} alternans and action potential (AP) duration alternans. Reduced RyR2 protein expression also resulted in cardiac hypertrophy and sudden death, as reported previously [20]. Our data suggest that reducing the protein expression of RyR2 may represent an effective approach for suppressing CPVT.

Experimental procedures

Animal studies

All animal studies were approved by the Institutional Animal Care and Use Committees at the University of Calgary and were performed in accordance with the US National Institutes of Health guidelines. The RyR2-targeted mutant mouse (*crr^{m1}*) was generated as described previously [19]. Adult homozygous *crr^{m1}* mutant mice and WT littermates (8–10 weeks) in the 129-E mouse background (Charles River) were used for all experiments. Note that in the study by Takeshima et al. [19], two RyR2 mutant mouse lines were generated: one is a RyR2-targeted mutant mouse called *crr^{m1}* and the other is a Cre-recombined RyR2 mutant mouse called *crr^{m2}*. In the *crr^{m1}* mutant mice, a *loxP* sequence was inserted into the 5'-untranslation region in exon 1, and a cassette containing a *loxP* sequence, the green fluorescence protein (GFP) cDNA, and the neomycin resistance gene (Neo) was inserted into the first intron of the mouse *rry2* gene. In the *crr^{m2}* mutant mice, the DNA sequence between the two *loxP* sites has been removed using the Cre-mediated recombination, resulting in the deletion of exon 1 and, thus, the RyR2 KO. Takeshima et al. used the *crr^{m2}* mutant mice to study the impact of RyR2 KO on the heart. In the present study, we used the *crr^{m1}* mutant mice without subjecting them to Cre-mediated recombination.

Western blot analysis

The *crr^{m1}* mutant and WT mouse hearts were frozen by a liquid N_2 -precooled Wollenberger clamp. The frozen heart tissues were ground to powder in the presence of liquid N_2 and homogenated in the homogenizing buffer (30 mM KH₂PO₄, pH 7.0, 40 mM NaF, 5 mM EDTA, 0.3 M sucrose, 4 $\mu\text{mol/l}$ leupeptin, 1 mM benzamidine, 100 $\mu\text{mol/l}$ PMSF, and 0.5 mM DTT) using a precooled Brinkmann Polytron PT 15 homogenizer. The cell homogenate (100 μl) was solubilized in a final 500 μl buffer containing 3% SDS and 50 mM Tris-HCl (pH 7.5) at room temperature for 1 h and incubated at 55°C for 10 min before centrifugation to remove unsolubilized materials. The solubilized proteins from WT or the *crr^{m1}* mutant hearts were separated by 6%, 8%, or 15% SDS-polyacrylamide gel electrophoresis (SDS-PAGE) and were transferred to nitrocellulose membranes at

100 V for 1.5 h at 4°C in the presence of 0.01% SDS [29,30]. The nitrocellulose membranes were then blocked for 1 h with phosphate-buffered saline (PBS: 137 mM NaCl, 8 mM Na₂HPO₄, 1.5 mM KH₂PO₄, and 2.7 mM KCl, pH 7.4) containing 0.5% Tween-20 and 5% skim milk powder. The membranes were incubated separately with the anti-RyR (34c, mouse), anti-Ca_v1.2 (rabbit), anti-SERCA (rabbit), anti-NCX (mouse), anti-CASQ2 (calsequestrin; rabbit), or anti-β-actin (rabbit) antibodies (Thermo Fisher Scientific) to detect the expression level of major Ca²⁺-handling proteins. The membranes were washed three times with PBS containing 0.5% Tween-20 for 15 min before incubating with the corresponding secondary anti-IgG antibodies conjugated with horseradish peroxidase (1 : 20 000) (Thermo Fisher Scientific) for 30 min. The detection of the bound antibodies was enhanced by the chemiluminescence kit from Pierce and visualized by ImageQuant LAS 4000 from GE Healthcare Life Sciences.

Hematoxylin and eosin staining

Hearts from the *crr*^{m1} mutant mice and their WT littermates were isolated and washed with Krebs–Ringers–HEPES (KRH) buffer (125 mM NaCl, 12.5 mM KCl, 25 mM HEPES, pH 7.4, 6 mM glucose, and 1.2 mM MgCl₂) and fixed with 4% paraformaldehyde solution via the retrograde Langendorff perfusion system. The fixed hearts were cut across the long axis to show the four chambers and then put into tissue cassettes. The dehydrating, clearing, and paraffining were performed using the Leica ASP300S tissue processor. The paraffin-embedded blocks were cut at 5 µm thick and mounted onto slides, air-dried for 30 min at room temperature and were baked at 37°C overnight. The paraffin sections were deparaffinized by xylene and rehydrated through ethanol and tap water before labeling with hematoxylin. Three minutes after stained with hematoxylin, the slides were rinsed in 1% acid alcohol (70%) several times to remove free hematoxylin and then were immersed in PBS for dark-blue color reaction product and thereafter, washed with distilled water and then stained with eosin for 3 min. The hematoxylin and eosin (H&E)-stained slides were dehydrated in alcohol, cleared in xylene, and mounted with coverslips. Photomicrographs were captured with a bright field microscope (Olympus BX53).

Electrocardiographic recordings and induction of cardiac arrhythmias in anesthetized mice

The *crr*^{m1} mutant and WT mice were lightly anesthetized with isoflurane vapor (0.5–1%) and 95% O₂, and placed on a heating pad (27°C). Two subcutaneous needle electrodes were inserted into the right upper limb and left lower abdomen for electrocardiographic (ECG) recordings (BIOPAC MP System, Goleta, CA). The ECGs were continuously monitored under anesthesia until heart rate became stable. Baseline ECGs were recorded for 5–10 min before stimulation. For induction of ventricular arrhythmias, mutant mice and their WT littermates were subjected to intraperitoneal injection of epinephrine (1.6 mg/kg) and caffeine (120 mg/kg) (low dose), or were injected with 3.0 mg/kg epinephrine and 150 mg/kg caffeine (high dose). ECGs were continuously recorded for 30 min after the infusion of epinephrine and caffeine [31].

Monophasic action potential recordings in Langendorff-perfused hearts

The *crr*^{m1} mutant and WT mice were killed by cervical dislocation. Their hearts were cannulated to a Langendorff apparatus for maintaining coronary perfusion with oxygenated Tyrode's buffer (118 mM NaCl, 5.4 mM KCl, 25 mM NaHCO₃, 1 mM MgCl₂, 0.42 mM NaH₂PO₄, 11.1 mM glucose, 10 mM taurine, and 5 mM creatine, pH 7.4) containing 1.8 mM Ca²⁺ at 35°C. A monophasic action potential (MAP) electrode was placed against the epicardial surface of the lower middle part of the left ventricle for epicardial MAP recording. Baseline MAP was recorded for 5–10 min before pacing at the right atrium from 5 to 10 Hz at 4–10 V for >20 s to induce AP duration (APD) alternans. The total length of the recording was 30 min. MAP signals were amplified by Gould amplifiers (models 13-G 4615-58, 13-4615-50 and 13-4615-71) and acquired at 2000 Hz/channel using a Data Translation (DT 2821) analog and digital input–output board. Analysis of MAP signals was performed using Acknowledgment (BIOPAC MP System, Goleta, CA).

Laser scanning confocal Ca²⁺ imaging of intact hearts

The *crr*^{m1} mutant mice and WT littermates were killed by cervical dislocation. Their hearts were cannulated to a Langendorff apparatus for maintaining coronary perfusion with oxygenated Ca²⁺-free Tyrode's buffer for 3–5 min and loaded with 4.4 µM Rhod-2 AM (Biotium, Inc., Hayward, CA) for ~45 min at 25°C [32,33].

Extracellular Ca^{2+} was stepwise introduced to the heart from 0.25, 0.5, 1.0, to 1.8 mM in the presence of 5 μM blebbistatin (Toronto Research Chemicals, Toronto, ON) at 35°C throughout the experiment. The Langendorff-perfused hearts were placed on a recording chamber mounted onto the Nikon A1R microscope for *in situ* confocal imaging (line-scan) of Ca^{2+} signals from epicardial ventricular myocytes. The pixel size of the resulting line-scan images ranged between 1.8 and 2 ms in the temporal dimension and between 0.1 and 0.4 μm in the spatial dimension. Ca^{2+} alternans was induced by rapid electrical stimulation of the hearts at increasing frequencies (5–12 Hz, 6 V). Data analysis was performed using the NikonA1R analysis system and Image J software.

Image and signal processing

The following signal and image processing methods were implemented using MATLAB (The Mathworks, Inc., Boston, MA) as described previously [34,35]. Briefly, line-scan fluorescence images were filtered using a median filter applied iteratively many times according to an estimation of the image noise variance. Noise variance was robustly estimated by means of a median absolute deviation of the image pixels. Identification of individual cells in the line-scan was performed by manually labeling the cell regions. Average fluorescence signals of individual cells in each line-scan were automatically obtained by spatial averaging of the pixels belonging to each marked cell. Average fluorescence signals of single cells were further filtered by applying a continuous wavelet transform of the signal with Gaussian wavelets of order 2. Zero-crossing of the derivative of the resulting wavelet transform was used to accurately locate peaks and valleys in the fluorescence signals. Peaks were then classified as either stimulated or spontaneous using cross-correlation with the stimulation pulse train. Peak amplitudes were defined as the difference between the peak and the corresponding previous valley. For each cell, alternans ratio was measured as the ratio of the absolute value of the difference in amplitude between two consecutive peaks over the amplitude of the largest peak. The presence of alternans periods was established by requiring at least six consecutive stimulated peaks presenting an alternans ratio above 0.05. For each cell, alternans duration was defined as the cumulative elapsed time of alternans periods over the total duration of the line-scan. The average alternans duration was determined by averaging alternans durations of all cells in one scan area; and the average alternans ratio was determined by averaging alternans ratios of cells that displayed alternans in the same scan area.

Echocardiography

Echocardiographic analysis of the WT and *crr^{m1}* mutant mice was carried out using the Vevo 770 echocardiography system equipped with a 30 MHz transducer probe (Visual Sonics, Toronto, Canada) as described recently [36]. Mice (8–9 weeks old) were gently constrained on a heating pad (37°C) and anesthetized with 1.5–2% isoflurane. Parameters, including the end systolic and diastolic diameters of the left chamber, interventricular septum and posterior wall thickness, left ventricular fractional shortening, and ejection fraction, were analyzed for each mouse in a blinded manner involving the B-mode and M-mode measurements. All data were averaged from 10 cardiac cycles per mouse.

Statistical analysis

All values shown are mean \pm SEM unless indicated otherwise. To test for differences between groups, we used unpaired Student's *t*-test (two-tailed) or one-way ANOVA with the post hoc test. A *P*-value of <0.05 was considered to be statistically significant.

Results

Modification of the *ryr2* gene for gene-targeted KO markedly reduces the protein expression of RyR2

During the process of generating the RyR2 KO mice, Takeshima et al. [19] previously produced a targeted mutant mouse (*crr^{m1}*), in which a *loxP* sequence was inserted into the 5'-untranslation region, and a cassette containing a *loxP* sequence, the GFP cDNA, and the Neo inserted into the first intron of the mouse *ryr2* gene (Figure 1A). Although these insertions in the intron sequences generally have a minimal impact on gene organization and expression, surprisingly, we found that homozygous *crr^{m1}* mutant mice displayed markedly reduced expression of the RyR2 protein. Immunoblotting analyses of whole heart lysates revealed that the expression level of the RyR2 protein in the *crr^{m1}* mutant hearts was substantially reduced compared with that in the WT

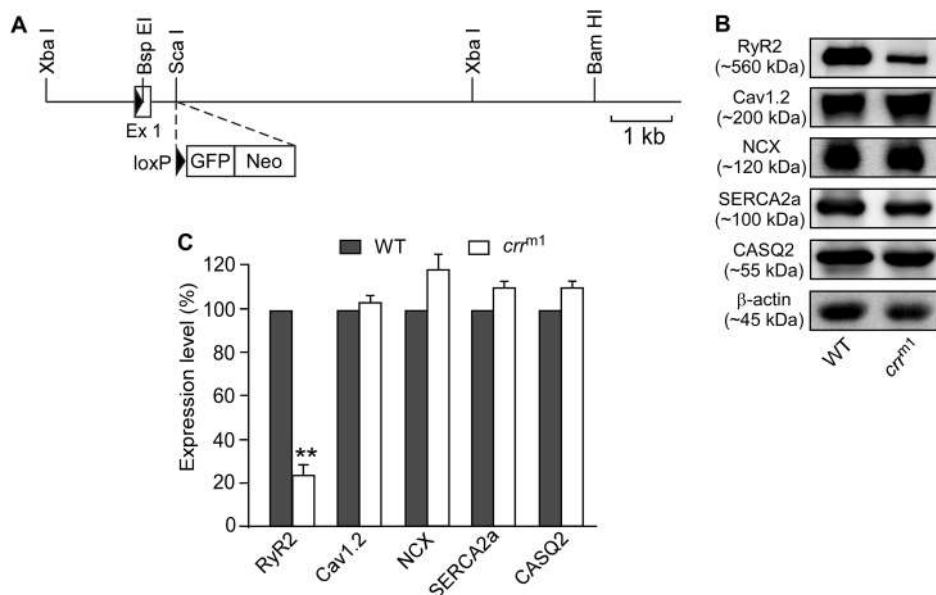


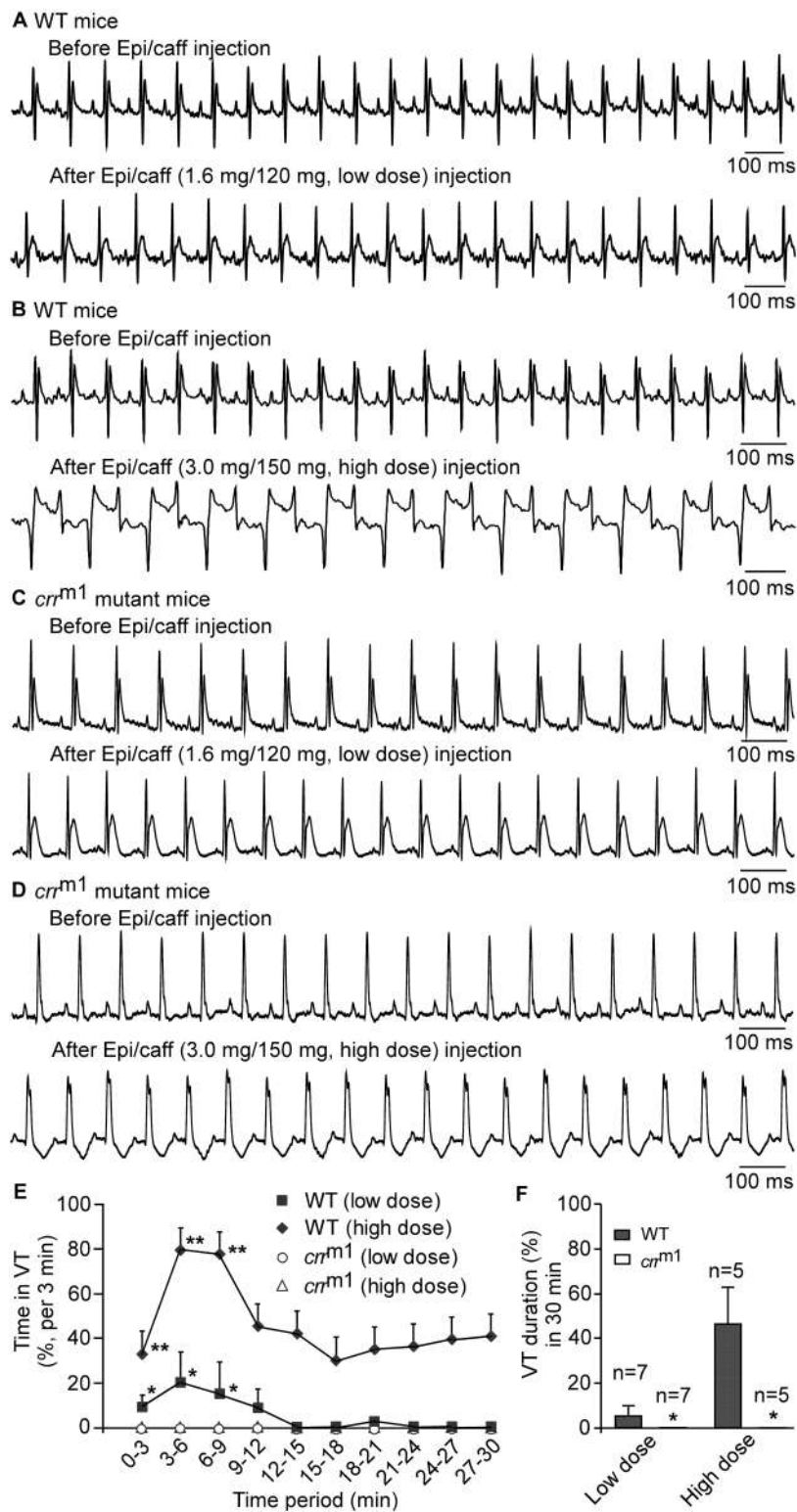
Figure 1. The *crr^{m1}* mutant mice display reduced RyR2 protein expression.

(A) Genetic manipulations in the mouse *ryr2* gene are illustrated [19]. The *loxP* sequence was introduced into the BspEI site in exon 1 (Ex 1) and the *loxP*-GFP-Neo cassette was inserted into the ScaI site in intron 1 after exon 1. (B) Western blot analysis of RyR2, Ca_v1.2, NCX, SERCA2a, CASQ2, and β-actin expression in the *crr^{m1}* mutant and WT hearts. The same amount of heart lysate proteins was loaded in each lane, and the bands were detected using the corresponding antibodies (*n* = 3–4). (C) The expression level of each protein in the *crr^{m1}* mutant hearts was normalized to that of the WT hearts. Data shown are mean ± SEM (*n* = 3–4) (***P* < 0.01).

hearts ($23.3 \pm 4.5\%$ vs. WT, $P < 0.01$) (Figure 1B,C). On the other hand, there were no significant differences in the expression levels of other major Ca²⁺-handling proteins between the *crr^{m1}* mutant and WT hearts, including the L-type Ca²⁺ channel, Na⁺/Ca²⁺ exchanger, SERCA, and CASQ2 (Figure 1B,C). Therefore, the *crr^{m1}* mutant mice express a markedly reduced level of RyR2 protein and represent a useful model for studying the impact of reduced RyR2 protein expression.

Reducing RyR2 protein expression protects against stress-induced ventricular tachyarrhythmia

It has been suggested that the level of RyR2 protein may play an important role in determining the susceptibility to CPVT [22,24,37]. However, direct evidence for the role of RyR2 protein expression in CPVT is lacking. To this end, we took advantage of the *crr^{m1}* mouse model to assess the impact of reduced RyR2 WT protein expression on stress-induced ventricular tachyarrhythmia (VT). We monitored the occurrence of VTs in WT and *crr^{m1}* mutant mice using ECG recordings before and after the injection of a mixture of caffeine (120 mg/kg) and epinephrine (1.6 mg/kg). This combination of pharmacological reagents has been widely used to trigger VTs in mouse models of CPVT [31,33,38–40]. Consistent with those reported previously, WT mice showed short durations of VTs ($5.7 \pm 4.1\%$) over the 30-min period of ECG recordings after the injection of these triggers (Figure 2A,E,F). Interestingly, not a single episode of VTs was detected in the *crr^{m1}* mutant mice under the same conditions (Figure 2C,E,F). These observations raise the possibility that the *crr^{m1}* mutant mice may be protected against stress-induced VTs. To test this hypothesis, we repeated the stress tests in WT and *crr^{m1}* mutant mice using higher doses of caffeine (150 mg/kg) and epinephrine (3.0 mg/kg). As expected, high doses of caffeine and epinephrine induced severe polymorphic and bidirectional VTs in WT mice, with an average VT duration of $46.3 \pm 16.0\%$ over the 30-min period of ECG recordings (Figure 2B,E,F). Remarkably, the *crr^{m1}* mutant mice showed no VTs at all after the injection of high doses of caffeine and epinephrine (Figure 2D,E,F). Thus, the *crr^{m1}* mutant mice are resistant to stress-induced VTs. Taken together, these observations indicate that reducing RyR2 WT protein expression can protect against stress-induced VTs in mice.

**Figure 2. The *crr^{m1}* mutant mice are resistant to stress-induced VTs.**

ECGs were recorded in anesthetized RyR2 WT and the *crr^{m1}* mutant mice. The mice were injected (i.p.) with 120 mg/kg caffeine plus 1.6 mg/kg epinephrine (low dose) or 150 mg/kg caffeine plus 3.0 mg/kg epinephrine (high dose). ECGs were recorded for another 30 min after injection. Representative ECG traces of the RyR2 WT mice (**A** and **B**) and the *crr^{m1}* mutant mice (**C** and **D**) before and after injection of low dose (**A** and **C**) or high dose (**B** and **D**) of caffeine and epinephrine. The VT

Part 1 of 2

Figure 2. The *crr^{m1}* mutant mice are resistant to stress-induced VTs.

Part 2 of 2

duration (%) in the RyR2 WT or the *crr^{m1}* mutant mice within each 3-min period (**E**) or within the 30-min period (**F**) of ECG recordings are shown. Data shown are mean \pm SEM ($n = 7$ for the low-dose group, $n = 5$ for the high-dose group) (* $P < 0.05$, ** $P < 0.01$).

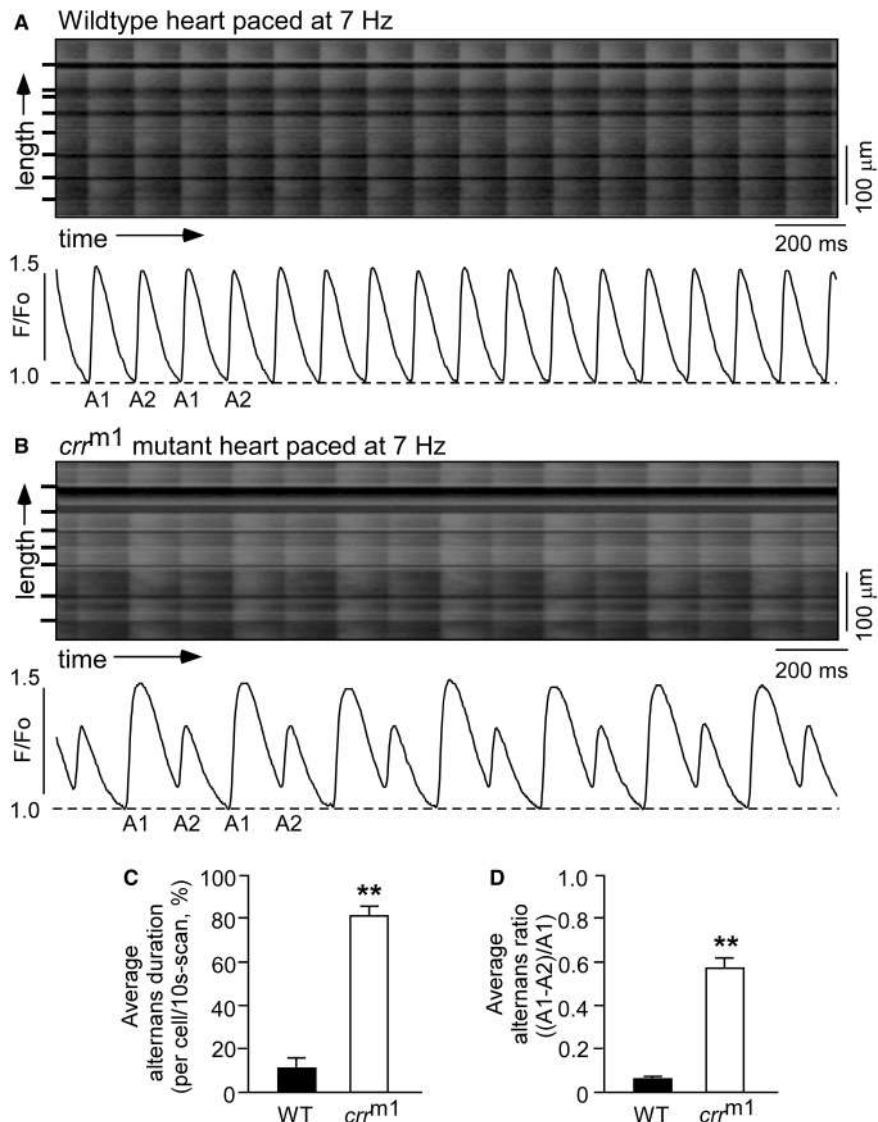


Figure 3. Ca^{2+} alternans in intact WT and *crr^{m1}* mutant hearts paced at 7 Hz.

Intact WT (**A**) and the *crr^{m1}* mutant (**B**) hearts were loaded with Rhod-2 AM and perfused with blebbistatin in a Langendorff setting. Ca^{2+} transients were elicited by pacing at 7 Hz and recorded using laser confocal imaging in the line-scanning mode. Cell boundaries were indicated by short bars on the left. The F/F_0 traces depict the average fluorescence signal of the scan area. Alternans duration for each cell in the scan area and alternans ratio for each cell that displayed alternans in the same scan area were determined and averaged per cell to yield the average alternans duration (**C**) and average alternans ratio (**D**). Alternans duration is defined as the percentage of time in alternans over the 10-s scanning period, and alternans ratio is defined as the ratio of the difference in amplitude between the large and small Ca^{2+} transients over the amplitude of the large Ca^{2+} transient. Data shown are mean \pm SEM ($n = 14$ scan areas from six WT hearts and $n = 20$ scan areas from seven *crr^{m1}* mutant hearts) (** $P < 0.01$).

Reducing RyR2 protein promotes Ca^{2+} alternans in intact hearts

We have previously shown that inhibiting the luminal Ca^{2+} activation of RyR2 suppresses stress-induced VTs, but enhances Ca^{2+} alternans [35]. It is possible that reducing the expression of the RyR2 protein, which suppresses stress-induced VTs, may also affect Ca^{2+} alternans. To test this possibility, we assessed the intracellular Ca^{2+} dynamics in intact working WT and the *crr^{m1}* mutant hearts stimulated at increasing frequencies (5–10 Hz) using *in situ* confocal laser scanning Ca^{2+} imaging. Figure 3 shows representative images and traces of Ca^{2+} transients obtained from WT and the *crr^{m1}* mutant hearts stimulated at 7 Hz. At this stimulation frequency, little or no Ca^{2+} alternans was detected in the WT hearts (Figure 3A), whereas the *crr^{m1}* mutant hearts showed severe Ca^{2+} alternans (Figure 3B). The average duration of Ca^{2+} alternans was $80.2 \pm 4.6\%$ in the *crr^{m1}* mutant hearts vs. $10.6 \pm 3.0\%$ in the WT hearts. The average alternans ratio was $57.3 \pm 4.4\%$ in the *crr^{m1}* mutant hearts vs. $5.8 \pm 1.7\%$ in the WT hearts (Figure 3C,D). Furthermore, the threshold stimulation frequency at which Ca^{2+} alternans occurred was lower in the *crr^{m1}* mutant hearts than in the WT hearts (Figure 4). Ca^{2+} alternans was readily detected in the *crr^{m1}* mutant hearts at a stimulation frequency of 5 Hz, whereas higher stimulation frequencies (8–10 Hz) were required to induce Ca^{2+} alternans in WT hearts (Figure 4). Moreover, the *crr^{m1}* mutant hearts displayed significantly longer alternans durations and higher alternans ratios at 5–10 Hz compared with the WT hearts at the same stimulation frequencies (Figure 4A,B). It should be noted that reducing RyR2 protein expression also affected the properties of Ca^{2+} transients. The *crr^{m1}* mutant hearts showed significantly increased time-to-peak and decay time (T_{50}), but similar amplitude of Ca^{2+} transients compared with WT hearts (Figure 5). Collectively, these observations indicate that reduced RyR2 protein expression enhances the susceptibility to Ca^{2+} alternans.

Reducing RyR2 protein enhances APD alternans

We next determined whether reduced RyR2 protein expression affects the propensity for APD alternans. MAP was recorded in Langendorff-perfused WT and the *crr^{m1}* mutant hearts. The hearts were stimulated with increasing frequencies from 5 to 10 Hz to induce APD alternans. As shown in Figure 6, WT hearts showed little or no APD alternans at the stimulation frequency of 8 Hz (Figure 6A), whereas the *crr^{m1}* mutant hearts exhibited significant APD alternans at the same stimulation frequency (8 Hz) (Figure 6B). As the stimulation frequency increased from 5 to 10 Hz, the ratios of APD alternans increased in both the WT and the *crr^{m1}* mutant hearts (Figure 6C). However, the APD alternans ratio in the *crr^{m1}* mutant hearts was significantly higher than that in the WT hearts at each stimulation frequency (between 6 and 10 Hz). For instance, at 8 Hz, the average APD alternans ratio was $2.6 \pm 0.9\%$ in WT hearts and $19.5 \pm 5.6\%$ in the *crr^{m1}* mutant hearts (Figure 6C). These results indicate that reduced RyR2 protein expression enhances the susceptibility to APD alternans.

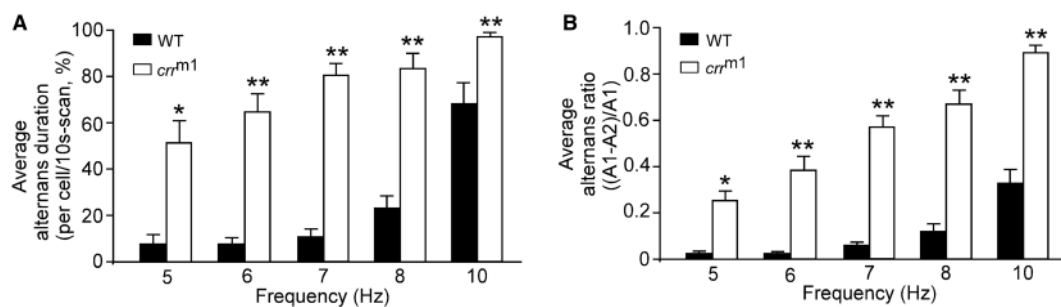


Figure 4. Average alternans duration and average alternans ratio at different pacing frequencies in intact WT and *crr^{m1}* mutant hearts.

Intact WT and *crr^{m1}* mutant hearts were loaded with Rhod-2 AM and perfused with blebbistatin in a Langendorff setting. Ca^{2+} transients were elicited by pacing at different frequencies from 5 to 10 Hz, and recorded using laser confocal imaging in the line-scanning mode. (A) Average alternans duration (%) in cells in WT or the *crr^{m1}* mutant hearts over the 10-s scanning period. (B) The average alternans ratio for cells that displayed alternans. Data shown are mean \pm SEM ($n = 14$ scan areas from six RyR2 WT hearts and $n = 20$ scan areas from seven *crr^{m1}* mutant hearts) (* $P < 0.05$, ** $P < 0.01$).

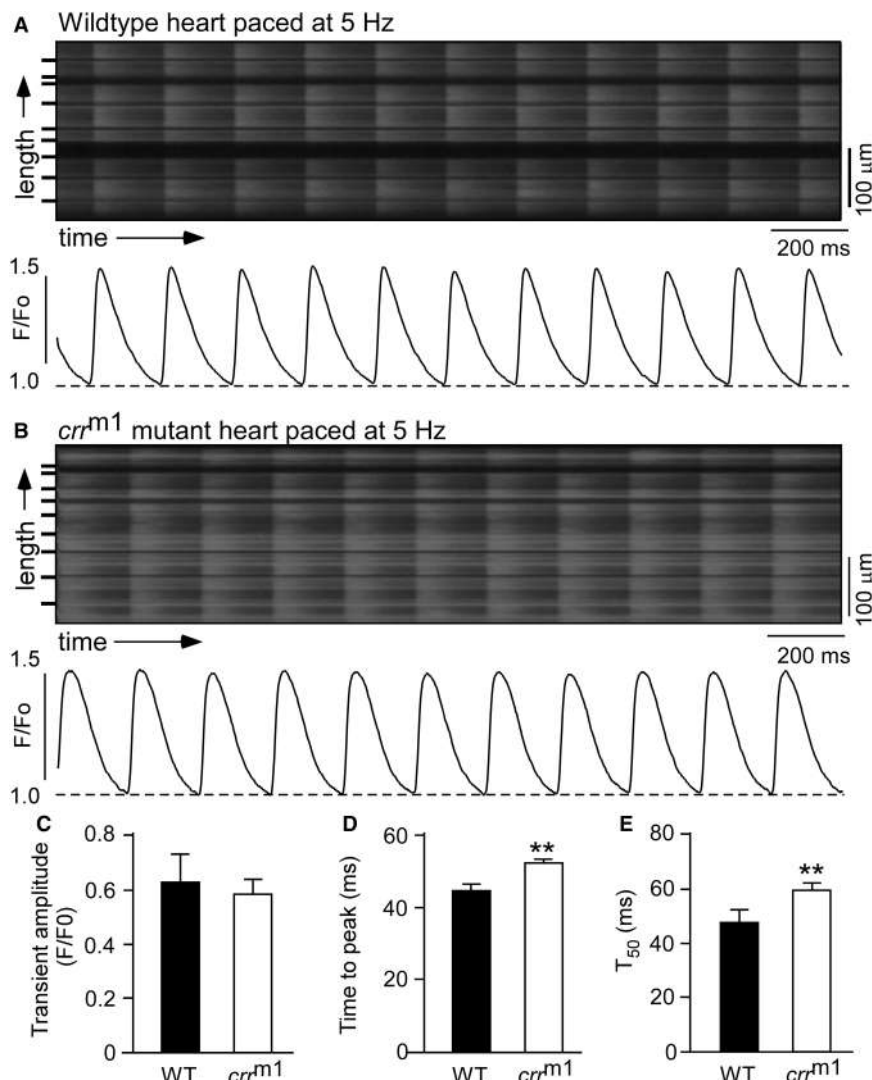


Figure 5. Ca^{2+} transient properties of the WT and crr^{m1} mutant hearts.

Intact WT (A) and the crr^{m1} mutant (B) hearts were loaded with Rhod-2 AM and perfused with blebbistatin in a Langendorff setting. Ca^{2+} transients were elicited by pacing at 5 Hz and recorded using laser confocal imaging in the line-scanning mode. Cell boundaries were indicated by short bars on the left. The F/F_0 traces depict the average fluorescence signal of the scan area. The average transient amplitude (C), time-to-peak (D), and decay time (T_{50}) of Ca^{2+} transients in the WT and crr^{m1} mutant hearts are indicated. Data shown are mean \pm SEM ($n = 4$ scan areas from two RyR2 WT hearts and $n = 13$ scan areas from seven crr^{m1} mutant hearts) (** $P < 0.01$).

The crr^{m1} mutant mice display cardiac hypertrophy and sudden death

Tissue-specific, conditional KO of RyR2 in the heart resulted in cardiac hypertrophy and sudden death [20]. To determine whether constitutively reducing RyR2 protein expression can lead to cardiac hypertrophy and sudden death, we assessed and compared the weights of the WT and crr^{m1} mutant hearts of the WT and crr^{m1} mutant mice. H&E staining of paraformaldehyde-fixed heart sections revealed increased thickness of the ventricular walls (Figure 7A) and ventricular cell area (Figure 7B,C) in the crr^{m1} mutant hearts compared with those in WT hearts. Consistent with these observations, echocardiographic analyses also revealed increased ventricular wall thickness in the crr^{m1} mutant hearts compared with the WT hearts (Table 1). Furthermore, the crr^{m1} mutant mice showed a significant increase in the heart-to-body-weight ratio compared with the WT mice ($56.0 \pm 2.8\%$ in crr^{m1} vs. $40.7 \pm 2.6\%$ in WT) (Figure 7D). Similar to that observed with the conditional

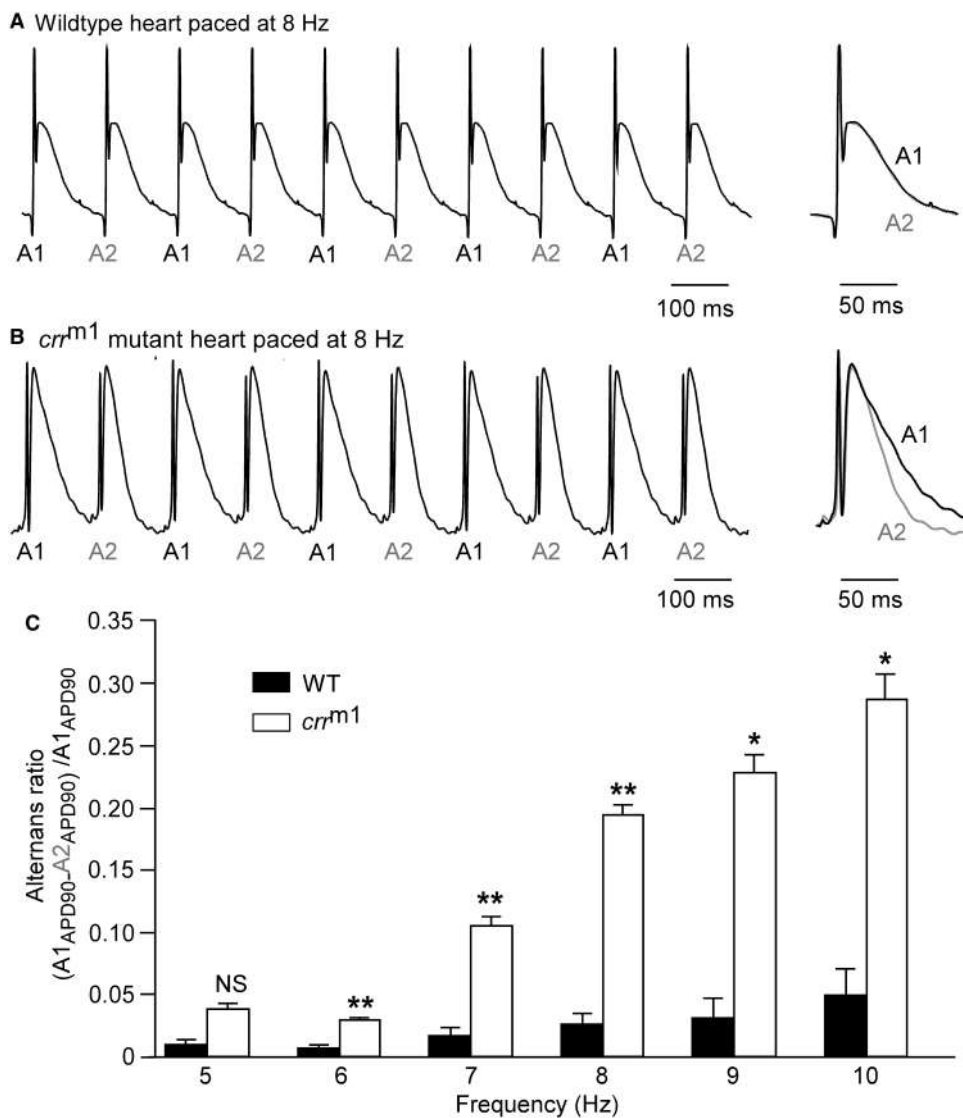


Figure 6. The *crr^{m1}* mutant hearts are more susceptible to APD alternans.

The WT and *crr^{m1}* mutant hearts were stimulated with increasing frequencies (5–10 Hz) at 5–10 V to induce APD alternans. Representative traces of MAP recordings from WT hearts (A) and the *crr^{m1}* mutant hearts (B) paced at 8 Hz are shown. (C) The APD alternans ratios of the WT and the *crr^{m1}* mutant hearts paced at different frequencies (5–10 Hz). Data shown are mean ± SEM ($n = 6$ for WT hearts and $n = 4$ for the *crr^{m1}* mutant hearts) (* $P < 0.05$, ** $P < 0.01$).

RyR2 KO mice [20], we also found that the *crr^{m1}* mutant mice exhibited sudden death at young ages, starting at ~40 days (Figure 8). On the other hand, no sudden death was observed with the WT mice (Figure 8). Taken together, these results indicate that reducing RyR2 protein expression can lead to cardiac hypertrophy and increase the incidence of sudden death.

Discussion

Although reduced RyR2 protein expression is likely to occur under various cardiac conditions, the impact of reduced RyR2 protein level on cardiac function is not well understood. In the present study, we exploited a mutant mouse model with reduced RyR2 protein expression. We found that reducing the protein expression of RyR2 suppresses stress-induced VTs, but enhances Ca^{2+} alternans and APD alternans. In addition, reduced

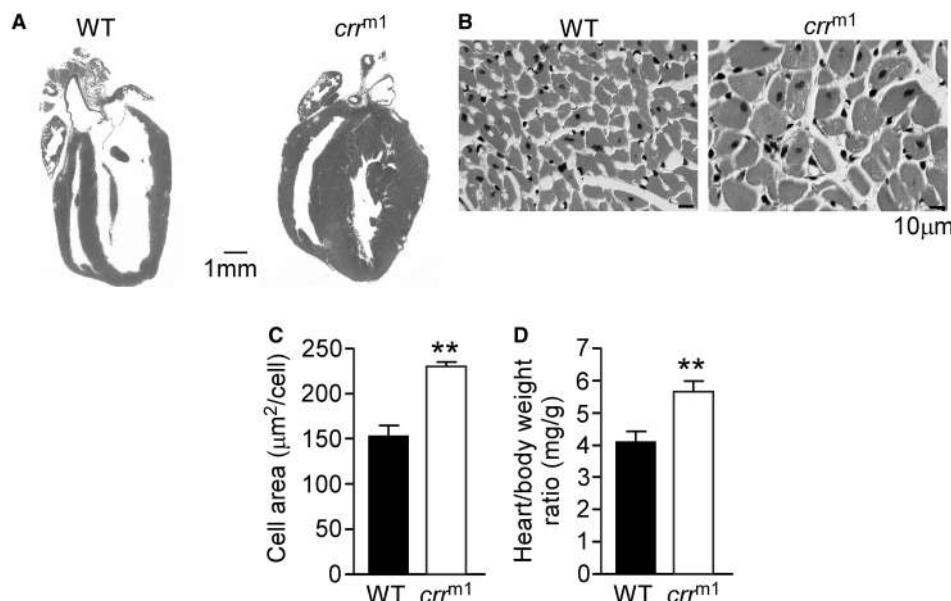


Figure 7. The *crr^{m1}* mutant mice show cardiac hypertrophy.

(A) Representative sections of the WT and *crr^{m1}* mutant hearts stained with H&E. (B) H&E-stained and transversal-sectioned myocardium from the free wall of the left ventricle. (C) The myocardium cell area in WT and *crr^{m1}* mutant hearts. (D) The heart- and body-weight ratios of the WT and *crr^{m1}* mutant hearts. Data shown are mean ± SEM ($n = 4$ for WT and $n = 6$ for *crr^{m1}* mutant mice) (** $P < 0.01$).

RyR2 protein expression led to cardiac hypertrophy and increased the susceptibility to sudden death. These findings provide novel insights into the role of RyR2 protein expression in VTs and cardiac alternans.

A remarkable finding from the present study is that mice with reduced RyR2 WT protein expression are resistant to stress-induced VTs, suggesting that the level of RyR2 WT protein expression can affect the propensity for stress-induced VTs. It has been shown that the severity of CPVT phenotypes in individuals with the same RyR2 mutations (e.g. deletion of exon-3 or G357S) can differ substantially [23,25–28]. Although the exact

Table 1 Echocardiographic analyses of WT and *crr^{m1}* mutant mice

Data shown are mean ± SEM.

	WT	<i>crr^{m1}</i>
LVS d (mm)	0.63 ± 0.02	0.84 ± 0.06*
LVS s (mm)	0.93 ± 0.04	1.20 ± 0.05*
LVPW d (mm)	0.73 ± 0.06	0.84 ± 0.05**
LVPW s (mm)	0.93 ± 0.03	1.19 ± 0.03*
FS (%)	31.63 ± 2.81	25.79 ± 3.6 ^{ns}
EF (%)	59.50 ± 4.02	50.65 ± 5.71 ^{ns}
Number of mice	10	6

Abbreviations: LVS d, interventricular septum thickness at end diastole; LVS s, interventricular septum thickness at end systole; LVPW d, left ventricular posterior wall thickness at end diastole; LVPW s, left ventricular posterior wall thickness at end systole; FS, fractional shortening; EF, ejection fraction.

* $P < 0.01$.

** $P < 0.05$.

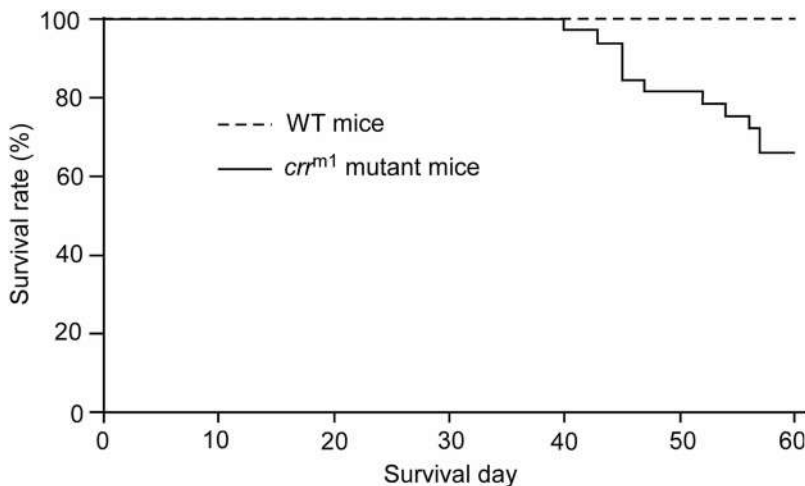


Figure 8. The *crr^{m1}* mutant mice died suddenly at young ages.

The survival rate of the *crr^{m1}* mutant mice ($n=32$) and the WT mice ($n=22$) is shown. Note that no WT mice died during the period (60 days) of observation, whereas the *crr^{m1}* mutant mice started to die at the age of 40 days.

mechanism underlying the phenotypic variability in the same families or in individuals with the same mutations is unknown, our finding suggests that reduced RyR2 protein expression may be one of the many factors that determine the penetrance of CPVT. It is possible that some CPVT-linked RyR2 mutations alter not only the gating properties of RyR2, but also its protein expression, which would, in turn, affect the propensity for CPVT. In support of this view, we have previously shown that deletion of exon-3 and the point mutation G357S markedly reduce the protein expression of RyR2, which may contribute to the incomplete penetrance of CPVT in individuals with these mutations [22–24]. Interestingly, Bongianino et al. [37] recently employed RNA interference to specifically reduce the protein expression of the RyR2 mutant allele in a CPVT mouse model expressing the RyR2 mutation R4496C. They found that allelic silencing of the RyR2 R4496C mutant expression is able to prevent CPVT in these mice. These observations suggest that reducing the expression of the RyR2 mutant protein represents a promising strategy for the treatment of CPVT. Our data would further suggest that reducing the expression level of the total RyR2 protein (both WT and mutant) may also be protective against CPVT. In this regard, it would be of great interest to determine whether individuals with nonsense or frame-shift RyR2 mutations that result in haploinsufficiency display reduced or enhanced susceptibility to CPVT.

It is important to note that suppressed RyR2 activity has been shown to enhance cardiac alternans [35]. Furthermore, reduced RyR2 protein expression has been implicated in the genesis of cardiac alternans [21]. Consistent with these observations, we found that reducing the protein expression of RyR2, indeed, increases the propensity for Ca^{2+} and AP duration alternans. Hence, although reducing the level of RyR2 protein expression can suppress stress-induced VTs, it can also increase the propensity for Ca^{2+} and APD alternans, a well-known cause of re-entrant arrhythmias that can lead to ventricular fibrillation and sudden death. Therefore, reducing the protein expression of RyR2 has the beneficial effect of suppressing stress-induced VTs, but the adverse effect of promoting cardiac alternans. Since cardiac alternans usually occurs at fast heart rates, one may be able to minimize the adverse effect of reduced RyR2 protein expression on cardiac alternans by controlling the heart rate. It is also important to note that reduced RyR2 protein expression also increases the risk of developing cardiac hypertrophy and sudden death [20]. Hence, a future challenge would be to fine tune the protein expression of RyR2, in addition to normalizing the activity of RyR2, in order to maximize its suppressing effect on stress-induced VTs, while minimize its adverse effect on cardiac alternans, hypertrophy, and sudden death.

The exact mechanism by which reducing RyR2 expression protects against stress-induced VTs, but promotes Ca^{2+} and APD alternans, is unknown. It has been shown that enhanced RyR2 function can increase the propensity for spontaneous SR Ca^{2+} release, which, in turn, can lead to delayed after depolarization, triggered activity, and VTs [2,3]. On the other hand, depressed RyR2 function can prolong the refractoriness of SR Ca^{2+} release, which, in turn, can increase the propensity for Ca^{2+} alternans [41–44]. Consistent with these

observations, we have previously shown that an RyR2 mutation E4872Q that reduces the activity of RyR2 by suppressing Ca^{2+} activation of the channel and spontaneous SR Ca^{2+} release protects against stress-induced VTs. On the other hand, the depressed E4872Q mutation prolongs the refractoriness of SR Ca^{2+} release and promotes Ca^{2+} alternans and APD alternans. It is likely that the rate of SR Ca^{2+} release would depend on the level of the RyR2 protein, such that reducing RyR2 protein expression to some extent may mimic the depression or reduction in RyR2 function. In line with this view, we found that reducing RyR2 protein expression, indeed, decreases the rate of rise of Ca^{2+} transients. Hence, it is possible that like the depressed RyR2 mutant E4872Q, reducing RyR2 protein expression may suppress spontaneous SR Ca^{2+} release and prolong SR Ca^{2+} release refractoriness. However, further investigations are needed to test these hypotheses.

In summary, the present study demonstrates that reducing the protein expression of RyR2 suppresses stress-induced VTs. This effect of reduced RyR2 protein expression on VTs may contribute to the incomplete penetrance of CPVT. Reduced RyR2 protein expression also increases the propensity for cardiac alternans, hypertrophy, and sudden death. Therefore, although moderate reduction in RyR2 protein expression may protect against CPVT, severe RyR2 protein reduction may lead to adverse effects.

Abbreviations

AF, atrial fibrillation; AP, action potential; APD, action potential duration; CASQ2, calsequestrin; CPVT, catecholaminergic polymorphic ventricular tachycardia; ECG, electrocardiography; GFP, green fluorescence protein; H&E, hematoxylin and eosin; KO, knockout; MAP, monophasic action potential; Neo, neomycin resistance gene; PBS, phosphate-buffered saline; RyR2, ryanodine receptor type 2; SERCA2a, sarco/endoplasmic reticulum Ca^{2+} ATPase; SR, sarcoplasmic reticulum; VT, ventricular tachyarrhythmia; WT, wild type.

Author Contribution

X.Z., A.V., B.S., Z.X., W.G., J.W., Y.C., E.R.O., A.M.G., L.H.-M., R.B., D.B., and S.R.W.C. designed the research. X.Z., B.S., Z.X., W.G., J.W., Y.C., and D.B. performed the research. X.Z., A.V., B.S., Z.X., J.W., M.N., Y.C., L.H.-M., R.B., D.B., and S.R.W.C. analyzed data. M.H. and H.T. provided research reagents, and X.Z., A.V., B.S., L.H.-M., R.B., and S.R.W.C. wrote the paper.

Funding

This work was supported by research grants from the Canadian Institutes of Health Research, the Heart and Stroke Foundation of Canada, the Canada Foundation for Innovation, and the Heart and Stroke Foundation Chair in Cardiovascular Research (to S.R.W.C.). The present study was also supported by the Spanish Ministry of Economy and Competitiveness [SAF2014-58286-C2-1-R] (L.H.-M.) and [DPI2013-44584-R] (R.B.).

Acknowledgements

We also like to thank Dr Long-Sheng Song, University of Iowa, for his continuous support and helpful discussion on intact heart Ca^{2+} imaging and the Libin Core Pathology Laboratory, Cumming School of Medicine, the University of Calgary, for H&E staining of the WT and mutant mouse heart tissues.

Competing Interests

The Authors declare that there are no competing interests associated with the manuscript.

References

- 1 Bers, D.M. (2002) Cardiac excitation–contraction coupling. *Nature* **415**, 198–205 <https://doi.org/10.1038/415198a>
- 2 Priori, S.G. and Chen, S.R.W. (2011) Inherited dysfunction of sarcoplasmic reticulum Ca^{2+} handling and arrhythmogenesis. *Circ. Res.* **108**, 871–883 <https://doi.org/10.1161/CIRCRESAHA.110.226845>
- 3 MacLennan, D.H. and Zvaritch, E. (2011) Mechanistic models for muscle diseases and disorders originating in the sarcoplasmic reticulum. *Biochim. Biophys. Acta, Mol. Cell Res.* **1813**, 948–964 <https://doi.org/10.1016/j.bbamcr.2010.11.009>
- 4 Ai, X., Curran, J.W., Shannon, T.R., Bers, D.M. and Pogwizd, S.M. (2005) Ca^{2+} /calmodulin-dependent protein kinase modulates cardiac ryanodine receptor phosphorylation and sarcoplasmic reticulum Ca^{2+} leak in heart failure. *Circ. Res.* **97**, 1314–1322 <https://doi.org/10.1161/01.RES.0000194329.41863.89>
- 5 Terentyev, D., Györke, I., Belevych, A.E., Terentyeva, R., Sridhar, A., Nishijima, Y. et al. (2008) Redox modification of ryanodine receptors contributes to sarcoplasmic reticulum Ca^{2+} leak in chronic heart failure. *Circ. Res.* **103**, 1466–1472 <https://doi.org/10.1161/CIRCRESAHA.108.184457>
- 6 Belevych, A.E., Radwański, P.B., Carnes, C.A. and Györke, S. (2013) 'Ryanopathy': causes and manifestations of RyR2 dysfunction in heart failure. *Cardiovasc. Res.* **98**, 240–247 <https://doi.org/10.1093/cvr/cvt024>

- 7 Jiang, D., Xiao, B., Zhang, L. and Chen, S.R. (2002) Enhanced basal activity of a cardiac Ca^{2+} release channel (ryanodine receptor) mutant associated with ventricular tachycardia and sudden death. *Circ. Res.* **91**, 218–225 <https://doi.org/10.1161/01.RES.0000028455.36940.5E>
- 8 Jiang, D., Xiao, B., Yang, D., Wang, R., Choi, P., Zhang, L. et al. (2004) RyR2 mutations linked to ventricular tachycardia and sudden death reduce the threshold for store-overload-induced Ca^{2+} release (SOICR). *Proc. Natl Acad. Sci. U.S.A.* **101**, 13062–13067 <https://doi.org/10.1073/pnas.0402388101>
- 9 Jiang, D., Wang, R., Xiao, B., Kong, H., Hunt, D.J., Choi, P. et al. (2005) Enhanced store overload-induced Ca^{2+} release and channel sensitivity to luminal Ca^{2+} activation are common defects of RyR2 mutations linked to ventricular tachycardia and sudden death. *Circ. Res.* **97**, 1173–1181 <https://doi.org/10.1161/01.RES.0000192146.85173.4B>
- 10 Jiang, D., Chen, W., Wang, R., Zhang, L. and Chen, S.R.W. (2007) Loss of luminal Ca^{2+} activation in the cardiac ryanodine receptor is associated with ventricular fibrillation and sudden death. *Proc. Natl Acad. Sci. U.S.A.* **104**, 18309–18314 <https://doi.org/10.1073/pnas.0706573104>
- 11 Jiang, D., Jones, P.P., Davis, D., Gow, R., Green, M., Birnie, D. et al. (2010) Characterization of a novel mutation in the cardiac ryanodine receptor that results in catecholaminergic polymorphic ventricular tachycardia. *Channels* **4**, 302–310 <https://doi.org/10.4161/chan.4.4.12666>
- 12 Tang, Y., Tian, X., Wang, R., Fill, M. and Chen, S.R.W. (2012) Abnormal termination of Ca^{2+} release is a common defect of RyR2 mutations associated with cardiomyopathies. *Circ. Res.* **110**, 968–977 <https://doi.org/10.1161/CIRCRESAHA.111.256560>
- 13 Naudin, V., Olivier, P., Rannou, F., Sainte Beuve, C. and Charlemagne, D. (1991) The density of ryanodine receptors decreases with pressure overload-induced rat cardiac hypertrophy. *FEBS Lett.* **285**, 135–138 [https://doi.org/10.1016/0014-5793\(91\)80743-M](https://doi.org/10.1016/0014-5793(91)80743-M)
- 14 Rannou, F., Dambrin, G., Marty, I., Carré, F., Trouvé, P., Lompré, A.M. et al. (1996) Expression of the cardiac ryanodine receptor in the compensated phase of hypertrophy in rat heart. *Cardiovasc. Res.* **32**, 258–265 [https://doi.org/10.1016/0008-6363\(96\)00095-8](https://doi.org/10.1016/0008-6363(96)00095-8)
- 15 Sainte Beuve, C., Allen, P.D., Dambrin, G., Rannou, F., Marty, I., Trouvé, P. et al. (1997) Cardiac calcium release channel (ryanodine receptor) in control and cardiomyopathic human hearts: mRNA and protein contents are differentially regulated. *J. Mol. Cell. Cardiol.* **29**, 1237–1246 <https://doi.org/10.1006/jmcc.1996.0360>
- 16 Yamamoto, T., Yano, M., Kohno, M., Hisaoka, T., Ono, K., Tanigawa, T. et al. (1999) Abnormal Ca^{2+} release from cardiac sarcoplasmic reticulum in tachycardia-induced heart failure. *Cardiovasc. Res.* **44**, 146–155 [https://doi.org/10.1016/S0008-6363\(99\)00200-X](https://doi.org/10.1016/S0008-6363(99)00200-X)
- 17 Voigt, N., Heijman, J., Wang, Q., Chiang, D.Y., Li, N., Karck, M. et al. (2014) Cellular and molecular mechanisms of atrial arrhythmogenesis in patients with paroxysmal atrial fibrillation. *Circulation* **129**, 145–156 <https://doi.org/10.1161/CIRCULATIONAHA.113.006641>
- 18 Chiang, D.Y., Kongchan, N., Beavers, D.L., Alsina, K.M., Voigt, N., Neilson, J.R. et al. (2014) Loss of microRNA-106b-25 cluster promotes atrial fibrillation by enhancing ryanodine receptor type-2 expression and calcium release. *Circ. Arrhythmia Electrophysiol.* **7**, 1214–1222 <https://doi.org/10.1161/CIRCEP.114.001973>
- 19 Takeshima, H., Komazaki, S., Hirose, K., Nishi, M., Noda, T. and Iino, M. (1998) Embryonic lethality and abnormal cardiac myocytes in mice lacking ryanodine receptor type 2. *EMBO J.* **17**, 3309–3316 <https://doi.org/10.1093/emboj/17.12.3309>
- 20 Bround, M.J., Asghari, P., Wambolt, R.B., Bohunek, L., Smits, C., Philit, M. et al. (2012) Cardiac ryanodine receptors control heart rate and rhythmicity in adult mice. *Cardiovasc. Res.* **96**, 372–380 <https://doi.org/10.1093/cvr/cvs260>
- 21 Wan, X., Laurita, K.R., Pruvot, E.J. and Rosenbaum, D.S. (2005) Molecular correlates of repolarization alternans in cardiac myocytes. *J. Mol. Cell. Cardiol.* **39**, 419–428 <https://doi.org/10.1016/j.jmcc.2005.06.004>
- 22 Liu, Y., Wang, R., Sun, B., Mi, T., Zhang, J., Mu, Y. et al. (2014) Generation and characterization of a mouse model harboring the exon-3 deletion in the cardiac ryanodine receptor. *PLoS ONE* **9**, e95615 <https://doi.org/10.1371/journal.pone.0095615>
- 23 Wangüemert, F., Bosch Calero, C., Pérez, C., Campuzano, O., Beltran-Alvarez, P., Scornik, F.S. et al. (2015) Clinical and molecular characterization of a cardiac ryanodine receptor founder mutation causing catecholaminergic polymorphic ventricular tachycardia. *Heart Rhythm* **12**, 1636–1643 <https://doi.org/10.1016/j.hrthm.2015.03.033>
- 24 Liu, Y., Wei, J., Wong King Yuen, S.M., Sun, B., Tang, Y., Wang, R. et al. (2017) CPVT-associated cardiac ryanodine receptor mutation G357S with reduced penetrance impairs Ca^{2+} release termination and diminishes protein expression. *PLoS ONE* **12**, e0184177 <https://doi.org/10.1371/journal.pone.0184177>
- 25 Bhuiyan, Z.A., van den Berg, M.P., van Tintelen, J.P., Bink-Boelkens, M.T.E., Wiesfeld, A.C.P., Alders, M. et al. (2007) Expanding spectrum of human RYR2-related disease: new electrocardiographic, structural, and genetic features. *Circulation* **116**, 1569–1576 <https://doi.org/10.1161/CIRCULATIONAHA.107.711606>
- 26 Medeiros-Domingo, A., Bhuiyan, Z.A., Tester, D.J., Hofman, N., Bikker, H., van Tintelen, J.P. et al. (2009) The RYR2-encoded ryanodine receptor/calcium release channel in patients diagnosed previously with either catecholaminergic polymorphic ventricular tachycardia or genotype negative, exercise-induced long QT syndrome: a comprehensive open reading frame mutational analysis. *J. Am. Coll. Cardiol.* **54**, 2065–2074 <https://doi.org/10.1016/j.jacc.2009.08.022>
- 27 Marjamaa, A., Lahtinen-Forsblom, P., Lahtinen, A.M., Viitasalo, M., Toivonen, L., Kontula, K. et al. (2009) Search for cardiac calcium cycling gene mutations in familial ventricular arrhythmias resembling catecholaminergic polymorphic ventricular tachycardia. *BMC Med. Genet.* **10**, 12 <https://doi.org/10.1186/1471-2350-10-12>
- 28 Ohno, S., Omura, M., Kawamura, M., Kimura, H., Itoh, H., Makiyama, T. et al. (2014) Exon 3 deletion of RYR2 encoding cardiac ryanodine receptor is associated with left ventricular non-compaction. *Europace* **16**, 1646–1654 <https://doi.org/10.1093/europace/eut382>
- 29 Laemmli, U.K. (1970) Cleavage of structural proteins during the assembly of the head of bacteriophage T4. *Nature* **227**, 680–685 <https://doi.org/10.1038/227680a0>
- 30 Towbin, H., Staehelin, T. and Gordon, J. (1979) Electrophoretic transfer of proteins from polyacrylamide gels to nitrocellulose sheets: procedure and some applications. *Proc. Natl Acad. Sci. U.S.A.* **76**, 4350–4434 <https://doi.org/10.1073/pnas.76.9.4350>
- 31 Zhou, Q., Xiao, J., Jiang, D., Wang, R., Vembaiyan, K., Wang, A. et al. (2011) Carvedilol and its new analogs suppress arrhythmogenic store overload-induced Ca^{2+} release. *Nat. Med.* **17**, 1003–1009 <https://doi.org/10.1038/nm.2406>
- 32 Chen, B., Guo, A., Gao, Z., Wei, S., Xie, Y.-P., Chen, S.R.W. et al. (2012) In situ confocal imaging in intact heart reveals stress-induced Ca^{2+} release variability in a murine catecholaminergic polymorphic ventricular tachycardia model of type 2 ryanodine receptor^{R449C/+} mutation. *Circ. Arrhythmia Electrophysiol.* **5**, 841–849 <https://doi.org/10.1161/CIRCEP.111.969733>
- 33 Chen, W., Wang, R., Chen, B., Zhong, X., Kong, H., Bai, Y. et al. (2014) The ryanodine receptor store-sensing gate controls Ca^{2+} waves and Ca^{2+} -triggered arrhythmias. *Nat. Med.* **20**, 184–192 <https://doi.org/10.1038/nm.3440>

- 34 Bai, Y., Jones, P.P., Guo, J., Zhong, X., Clark, R.B., Zhou, Q. et al. (2013) Phospholamban knockout breaks arrhythmogenic Ca^{2+} waves and suppresses catecholaminergic polymorphic ventricular tachycardia in mice. *Circ. Res.* **113**, 517–526 <https://doi.org/10.1161/CIRCRESAHA.113.301678>
- 35 Zhong, X., Sun, B., Vallmitjana, A., Mi, T., Guo, W., Ni, M. et al. (2016) Suppression of ryanodine receptor function prolongs Ca^{2+} release refractoriness and promotes cardiac alternans in intact hearts. *Biochem. J.* **473**, 3951–3964 <https://doi.org/10.1042/BCJ20160606>
- 36 Brodehl, A., Belke, D.D., Garnett, L., Martens, K., Abdelfatah, N., Rodriguez, M. et al. (2017) Transgenic mice overexpressing desmocollin-2 (DSC2) develop cardiomyopathy associated with myocardial inflammation and fibrotic remodeling. *PLoS ONE* **12**, e0174019 <https://doi.org/10.1371/journal.pone.0174019>
- 37 Bongianino, R., Denegri, M., Mazzanti, A., Lodola, F., Vollero, A., Boncompagni, S. et al. (2017) Allele specific silencing of mutant mRNA rescues ultrastructural and arrhythmic phenotype in mice carriers of the R4496C mutation in the ryanodine receptor gene (*RYR2*). *Circ. Res.* **121**, 525–536 <https://doi.org/10.1161/CIRCRESAHA.117.310882>
- 38 Priori, S.G., Napolitano, C., Tiso, N., Memmi, M., Vignati, G., Bloise, R. et al. (2001) Mutations in the cardiac ryanodine receptor gene (hRyR2) underlie catecholaminergic polymorphic ventricular tachycardia. *Circulation* **103**, 196–200 <https://doi.org/10.1161/01.CIR.103.2.196>
- 39 Zhang, J., Chen, B., Zhong, X., Mi, T., Guo, A., Zhou, Q. et al. (2014) The cardiac ryanodine receptor luminal Ca^{2+} sensor governs Ca^{2+} waves, ventricular tachyarrhythmias and cardiac hypertrophy in calsequestrin-null mice. *Biochem. J.* **461**, 99–106 <https://doi.org/10.1042/BJ20140126>
- 40 Zhang, J., Zhou, Q., Smith, C.D., Chen, H., Tan, Z., Chen, B. et al. (2015) Non- β -blocking R-carvedilol enantiomer suppresses Ca^{2+} waves and stress-induced ventricular tachyarrhythmia without lowering heart rate or blood pressure. *Biochem. J.* **470**, 233–242 <https://doi.org/10.1042/BJ20150548>
- 41 Diaz, M.E., Eisner, D.A. and O'Neill, S.C. (2002) Depressed ryanodine receptor activity increases variability and duration of the systolic Ca^{2+} transient in rat ventricular myocytes. *Circ. Res.* **91**, 585–593 <https://doi.org/10.1161/01.RES.0000035527.53514.C2>
- 42 Pieske, B. and Kockskämper, J. (2002) Alternans goes subcellular: a ‘disease’ of the ryanodine receptor? *Circ. Res.* **91**, 553–555 <https://doi.org/10.1161/01.RES.0000036862.37203.F4>
- 43 Picht, E., DeSantiago, J., Blatter, L.A. and Bers, D.M. (2006) Cardiac alternans do not rely on diastolic sarcoplasmic reticulum calcium content fluctuations. *Circ. Res.* **99**, 740–748 <https://doi.org/10.1161/01.RES.0000244002.88813.91>
- 44 Wang, L., Myles, R.C., De Jesus, N.M., Ohlendorf, A.K.P., Bers, D.M. and Ripplinger, C.M. (2014) Optical mapping of sarcoplasmic reticulum Ca^{2+} in the intact heart: ryanodine receptor refractoriness during alternans and fibrillation. *Circ. Res.* **114**, 1410–1421 <https://doi.org/10.1161/CIRCRESAHA.114.302505>